

## Probing the Energy-Smeared $R$ Ratio Using Lattice QCD

Constantia Alexandrou,<sup>1,2</sup> Simone Bacchio,<sup>2</sup> Alessandro De Santis,<sup>3</sup> Petros Dimopoulos,<sup>4</sup>  
 Jacob Finkenrath,<sup>2</sup> Roberto Frezzotti,<sup>3</sup> Giuseppe Gagliardi,<sup>5</sup> Marco Garofalo,<sup>6</sup> Kyriakos Hadjiyiannakou,<sup>1,2</sup>  
 Bartosz Kostrzewa,<sup>7</sup> Karl Jansen,<sup>8</sup> Vittorio Lubicz,<sup>9</sup> Marcus Petschlies,<sup>6</sup> Francesco Sanfilippo,<sup>5</sup> Silvano Simula,<sup>5</sup>  
 Nazario Tantalo<sup>3,\*</sup>, Carsten Urbach,<sup>6</sup> and Urs Wenger<sup>10</sup>

(Extended Twisted Mass Collaboration (ETMC))

<sup>1</sup>*Department of Physics, University of Cyprus, 20537 Nicosia, Cyprus*

<sup>2</sup>*Computation-based Science and Technology Research Center, The Cyprus Institute,  
 20 Konstantinou Kavafi Street, 2121 Nicosia, Cyprus*

<sup>3</sup>*Dipartimento di Fisica and INFN, Università di Roma Tor Vergata, Via della Ricerca Scientifica 1, I-00133 Roma, Italy*

<sup>4</sup>*Dipartimento di Scienze Matematiche, Fisiche e Informatiche, Università di Parma and INFN,  
 Gruppo Collegato di Parma, Parco Area delle Scienze 7/a (Campus), 43124 Parma, Italy*

<sup>5</sup>*Istituto Nazionale di Fisica Nucleare, Sezione di Roma Tre, Via della Vasca Navale 84, I-00146 Rome, Italy*

<sup>6</sup>*HISKP (Theory), Rheinische Friedrich-Wilhelms-Universität Bonn, Nussallee 14-16, 53115 Bonn, Germany*

<sup>7</sup>*High Performance Computing and Analytics Lab, Rheinische Friedrich-Wilhelms-Universität Bonn,  
 Friedrich-Hirzebruch-Allee 8, 53115 Bonn, Germany*

<sup>8</sup>*NIC, DESY, Platanenallee 6, D-15738 Zeuthen, Germany*

<sup>9</sup>*Dipartimento di Matematica e Fisica, Università Roma Tre and INFN, Sezione di Roma Tre,  
 Via della Vasca Navale 84, I-00146 Rome, Italy*

<sup>10</sup>*Institute for Theoretical Physics, Albert Einstein Center for Fundamental Physics,  
 University of Bern, Sidlerstrasse 5, CH-3012 Bern, Switzerland*



(Received 18 January 2023; revised 13 May 2023; accepted 18 May 2023; published 15 June 2023)

We present a first-principles lattice QCD investigation of the  $R$  ratio between the  $e^+e^-$  cross section into hadrons and into muons. By using the method of Ref. [1], that allows one to extract smeared spectral densities from Euclidean correlators, we compute the  $R$  ratio convoluted with Gaussian smearing kernels of widths of about 600 MeV and central energies from 220 MeV up to 2.5 GeV. Our theoretical results are compared with the corresponding quantities obtained by smearing the KNT19 compilation [2] of  $R$ -ratio experimental measurements with the same kernels and, by centering the Gaussians in the region around the  $\rho$ -resonance peak, a tension of about 3 standard deviations is observed. From the phenomenological perspective, we have not included yet in our calculation QED and strong isospin-breaking corrections, and this might affect the observed tension. From the methodological perspective, our calculation demonstrates that it is possible to study the  $R$  ratio in Gaussian energy bins on the lattice at the level of accuracy required in order to perform precision tests of the standard model.

DOI: [10.1103/PhysRevLett.130.241901](https://doi.org/10.1103/PhysRevLett.130.241901)

*Introduction.*—The  $R$  ratio between the  $e^+e^-$  cross section into hadrons with that into muons plays a fundamental rôle in particle physics since its introduction in Ref. [3]. In recent years, the importance of the  $R$  ratio has been mainly associated with the fact that its knowledge, as a function of the center-of-mass energy of the electrons, allows one to predict the leading hadronic contribution

(HVP) to the muon anomalous magnetic moment ( $a_\mu$ ) via a dispersive approach. The dispersive determinations of  $a_\mu^{\text{HVP}}$ , reviewed in detail in Ref. [4], are in strong tension (about 4 standard deviations) with the experimental determination of  $a_\mu$ . On the other hand, lattice determinations of (partial) contributions to  $a_\mu^{\text{HVP}}$ , obtained without any reference to the experimental measurements of  $R$ , are in much better agreement with the  $a_\mu$  experiment [5].

The focus of this Letter is  $R$ , smeared with Gaussian kernels, and not  $a_\mu$ .—The experiments that measure  $R$  are radically different from those that measure  $a_\mu$ , and moreover,  $R$  is an energy-dependent probe of the theory while  $a_\mu$  is natively a low-energy observable. For these reasons a

---

*Published by the American Physical Society under the terms of the Creative Commons Attribution 4.0 International license. Further distribution of this work must maintain attribution to the author(s) and the published article's title, journal citation, and DOI. Funded by SCOAP<sup>3</sup>.*

detailed phenomenological investigation of  $R$  represents an independent precision test of the standard model with respect to that provided by  $a_\mu$ . We address here the theoretical side of this problem by computing the energy-smeared  $R$  ratio on the lattice with the required nonperturbative accuracy.

To this end, we rely on our effort within the ETMC that produced a collection of state-of-the-art lattice QCD ensembles with four dynamical twisted mass quark flavors [6] at physical pion masses together with the Euclidean correlators with two insertions of the hadronic electromagnetic current (see Table I and Ref. [7]). From these correlators, by using the method proposed in Ref. [1] and recently validated in Ref. [8] (see also Ref. [9]), we extract the  $R$  ratio smeared with normalized Gaussian kernels,  $G_\sigma(\omega) = \exp(-\omega^2/2\sigma^2)/\sqrt{2\pi\sigma^2}$ , according to

$$R_\sigma(E) = \int_0^\infty d\omega G_\sigma(E - \omega)R(\omega). \quad (1)$$

We then compare our theoretical determinations of  $R_\sigma(E)$  with experiments by smearing the  $R$  measurements with the same Gaussian. In this way, by varying  $E$  and  $\sigma$ , we probe  $R$  in Gaussian energy bins of different widths (see also Ref. [10]). With  $E$  around the  $\rho$ -resonance peak and at  $\sigma \simeq 600$  MeV we manage to compute  $R_\sigma(E)$  with an accuracy at the 2% level. In these Gaussian bins our results are in tension (about 3 standard deviations) with experiments.

From the phenomenological perspective, the observed tension might be ascribed to QED and strong isospin-breaking effects, which we have not included yet in our isosymmetric QCD calculation, or to underestimated experimental uncertainties (see, e.g., Ref. [11]). From the methodological viewpoint, our results clearly demonstrate that it is possible to study the  $R$  ratio in Gaussian energy bins on the lattice at the precision level required to perform precision tests of the standard model.

A resolution in energy of  $O(600)$  MeV can also be obtained by considering the so-called intermediate window contribution ( $a_\mu^{\text{HVP},W}$ ) to  $a_\mu$ . Presently, the comparison of the lattice determinations [5,7,12,13] of  $a_\mu^{\text{HVP},W}$  with the corresponding dispersive determinations [2] represents a more stringent test of the standard model with respect to the one performed in this Letter. Having demonstrated here that a precise lattice calculation of  $R_\sigma(E)$  is possible, we plan in the near future to substantially reduce the widths of the Gaussian bins by increasing the statistical precision of our lattice correlators.

*Methods and materials.*—Methods:—In order to compute  $R_\sigma(E)$  we start from the two-point Euclidean correlator of the quark electromagnetic current

$$V(t) = -\frac{1}{3} \sum_{i=1}^3 \int d^3x T \langle 0 | J_i(x) J_i(0) | 0 \rangle, \quad (2)$$

where  $J_\mu = \sum_f q_f \bar{\psi}_f \gamma_\mu \psi_f$  with  $f = \{u, d, s, c, b, t\}$ ,  $q_{u,c,t} = 2/3$ , and  $q_{d,s,b} = -1/3$ . These correlators are the primary data of our lattice simulations and are connected to the  $R$  ratio by the well-known formula

$$V(t) = \frac{1}{12\pi^2} \int_0^\infty d\omega \omega^2 R(\omega) e^{-t\omega}. \quad (3)$$

Theoretically  $R(\omega)$  is a distribution, the spectral density of the correlator  $V(t)$ , and it *has* to be probed by using suitable smearing kernels,

$$R[K] = \int_0^\infty d\omega K(\omega) R(\omega). \quad (4)$$

In this perspective the correlator  $V(t)$  itself represents a class of observables, corresponding to  $K(\omega) = \omega^2 \exp(-t\omega)/12\pi^2$ , whose sensitivity to the energy dependence of  $R$  can be varied by changing  $t$ . The window contributions [14] to  $a_\mu^{\text{HVP}}$  are elements of another class of observables whose smearing kernels are natively well localized in the Euclidean-time domain (see, e.g., Figs. 1 and 2 of Ref. [7]), but that can also be used to probe the energy dependence of  $R(E)$  by changing the parameters that define the time window (see Ref. [15] and Fig. 6 below). By choosing  $K(\omega) = G_\sigma(E - \omega)$  we provide here results for  $R_\sigma(E)$ , a class of observables that are natively well localized in the energy domain.

The determination of  $R_\sigma(E)$  on the lattice is possible, with controlled statistical and systematic errors, by using the method [16] of Ref. [1]. The starting point of this approach is the following exact representation of the smearing kernel for  $\omega > 0$ :

$$\frac{12\pi^2 G_\sigma(E - \omega)}{\omega^2} = \sum_{\tau=1}^\infty g_\tau e^{-a\omega\tau}, \quad (5)$$

where  $\tau$  is an integer variable and  $a$  is an arbitrary scale that, on the lattice, we identify with the lattice spacing. Once the coefficients  $g_\tau \equiv g_\tau(E, \sigma)$  are known,  $R_\sigma(E)$  can be computed according to

$$R_\sigma(E) = \sum_{\tau=1}^\infty g_\tau V(a\tau). \quad (6)$$

Although the mathematics is quite simple the game is rather delicate from the numerical point of view. Indeed, since the sums in Eqs. (5) and (6) have necessarily to be truncated, the goal is to find a finite set of coefficients such that both the systematic and statistical errors on the resulting approximation to  $R_\sigma(E)$  can be kept under control. The smoother the kernel is, the simpler the game is. The numerical problem rapidly becomes ill posed for  $\sigma \ll E$  (see Refs. [1,8] for illustrative numerical evidence of this fact). In this regime, any procedure aiming at minimizing the systematic error due to the imperfect reconstruction of

TABLE I. ETMC gauge ensembles used in this Letter. The quoted pion masses have been obtained by a direct computation of the small light-quark mass correction that is necessary to match  $m_\pi = 135.0$  MeV starting from simulations with slightly heavier pions [ $m_\pi = 0.1402(2)$  GeV on the B64 ensemble,  $m_\pi = 0.1401(1)$  GeV on the B96 ensemble,  $m_\pi = 0.1367(2)$  GeV on the C80 ensemble, and  $m_\pi = 0.1408(2)$  GeV on the D96 ensemble; see Ref. [7] for more details].

ID	$L^3 \times T$	$a$ fm	$aL$ fm	$m_\pi$ GeV
B64	$64^3 \times 128$	0.07957(13)	5.09	0.1352(2)
B96	$96^3 \times 192$	0.07957(13)	7.64	0.1352(2)
C80	$80^3 \times 160$	0.06821(13)	5.46	0.1349(3)
D96	$96^3 \times 192$	0.05692(12)	5.46	0.1351(3)

the kernel produces coefficients  $g_\tau$  that are huge in magnitude and oscillating in sign. As a consequence, any tiny error on  $V(a\tau)$  is amplified when the truncated sum of Eq. (6) is evaluated. The algorithm of Ref. [1] provides a regularization mechanism to this problem. We refer to Refs. [1,8] for extended discussions of this point and to the Supplemental Material [22] for the details of the numerical implementation performed in this Letter.

Materials:—The lattice gauge ensembles used in this Letter, generated by the ETMC, are listed in Table I and described in full details in Ref. [7] together with the lattice correlators  $V(t)$ , used there to compute the short and intermediate window contributions to  $a_\mu^{\text{HVP}}$  and here to compute  $R_\sigma(E)$ . In particular, in order to better estimate the systematics associated with continuum extrapolations, we use the same mixed-action setup described in Ref. [7,27] and analyze both the so-called twisted mass (TM) and Osterwalder-Seiler (OS) lattice regularized correlators  $V(t)$ . The results for  $R_\sigma(E)$  obtained in the two regularizations differ by  $O(a^2)$  cutoff effects [28,29] and must coincide within errors in the continuum limit.

In order to compare our theoretical results with experiments, we rely on the KNT19 compilation [2] of  $R_\sigma^{\text{exp}}(E)$ , providing data in the range  $E \in [0.216, 11.1985]$  GeV together with the full covariance matrix that takes into account the correlation between the different experiments; see Fig. 1. The central values and errors of  $R_\sigma^{\text{exp}}(E)$  quoted below have been obtained by generating bootstrap samples of  $R(E)$ , each of which simulating an independent measurement, from a multivariate Gaussian distribution using the  $R^{\text{exp}}(\omega)$  central values and covariance matrix. Each sample is then integrated with  $G_\sigma(E - \omega)$ ; see the Supplemental Material [22] for more details.

Results.—In our lattice calculation we considered three values for the smearing parameter,  $\sigma = \{0.44, 0.53, 0.63\}$  GeV, and central energies in the range  $E \in [0.21, 2.54]$  GeV. A detailed discussion of the analysis procedure, including the breakdown of  $R_\sigma(E)$  into the contributions coming from the different flavors and from

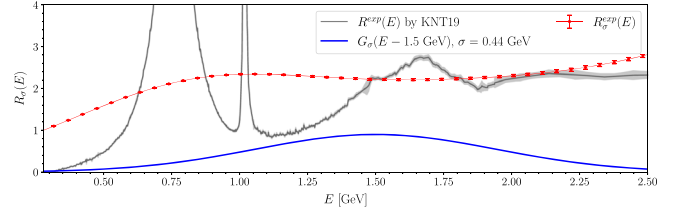


FIG. 1. The gray band shows  $R_\sigma^{\text{exp}}(E)$  from the KNT19 compilation [2]. The red points are the results of the smearing of  $R_\sigma^{\text{exp}}(E)$  with a Gaussian of  $\sigma = 0.44$  GeV according to Eq. (1). The smearing Gaussian corresponding to center energy  $E = 1.5$  GeV is shown in blue.

connected and disconnected fermionic Wick contractions, together with a careful study of the systematic uncertainties affecting each contribution, can be found in the Supplemental Material [22]. Here, in Fig. 2, we show an

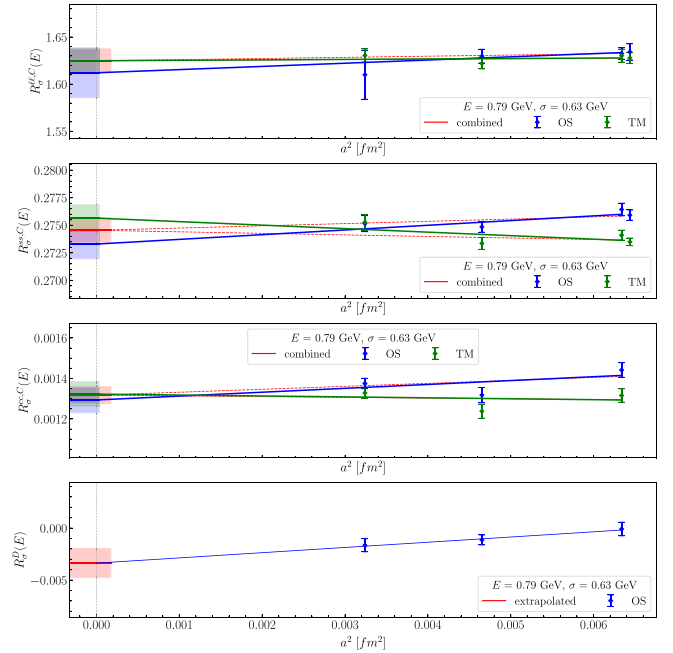


FIG. 2. Continuum extrapolations of the different contributions to  $R_\sigma(E)$  at  $E = 0.79$  GeV and  $\sigma = 0.63$  GeV. From top to bottom, the plots correspond to the connected light-light [ $R_\sigma^{\ell\ell,C}(E)$ ], the connected strange-strange [ $R_\sigma^{ss,C}(E)$ ], the connected charm-charm [ $R_\sigma^{cc,C}(E)$ ] and the disconnected [ $R_\sigma^D(E)$ ] contributions. The blue and green points correspond respectively to the OS and TM lattice regularizations. In the case of the connected contributions we performed both correlated-constrained (red) and uncorrelated-unconstrained linear extrapolations in  $a^2$  and found them to be compatible within errors in all cases. The disconnected contribution has been computed in the OS regularization only and extrapolated linearly in  $a^2$ . In the case of  $R_\sigma^{\ell\ell,C}(E)$  and  $R_\sigma^{ss,C}(E)$  there are two points for each regularization at the coarsest lattice spacing (slightly displaced on the  $x$  axis to help the eye) corresponding to the ensembles B64 and B96 and, therefore, to different volumes. No significant finite-volume effects have been observed for all considered values of  $E$  and  $\sigma$ .

example ( $E = 0.79$  GeV and  $\sigma = 0.63$  GeV) of the continuum extrapolations of the different contributions to  $R_\sigma(E)$  and, in the following, concentrate on the comparison of our first-principles determination with the experimental results  $R_\sigma^{\text{exp}}(E)$ .

This is done in Fig. 3 where the plots show  $R_\sigma(E)$  (blue points) and  $R_\sigma^{\text{exp}}(E)$  (red points) as functions of  $E$  for  $\sigma = 0.44$  GeV (first row),  $\sigma = 0.53$  GeV (second row), and  $\sigma = 0.63$  GeV (third row). Our quoted final errors include the estimates of the systematics associated with continuum extrapolations, with finite-volume effects and also the ones coming from the spectral reconstruction algorithm; see Fig. 4. In order to properly interpret Fig. 3 it is very important to realize that the information contained in  $R_\sigma(E)$  and  $R_\sigma(E')$  for central energies such that  $|E - E'| \ll \sigma$  is essentially the same. Moreover, our theoretical results at different values of  $E$  and  $\sigma$  are obtained from the same correlators and, therefore, are correlated (a table with the numerical results and their correlation matrix is provided in the Supplemental Material [22]). It is also very important to stress that our lattice simulations have been calibrated by using hadron masses to fix the quark masses and the lattice spacing, and therefore,  $R_\sigma(E)$  is a theoretical prediction obtained without using any input coming from  $R_\sigma^{\text{exp}}(E)$ . In view of these observations, and of the fact that the

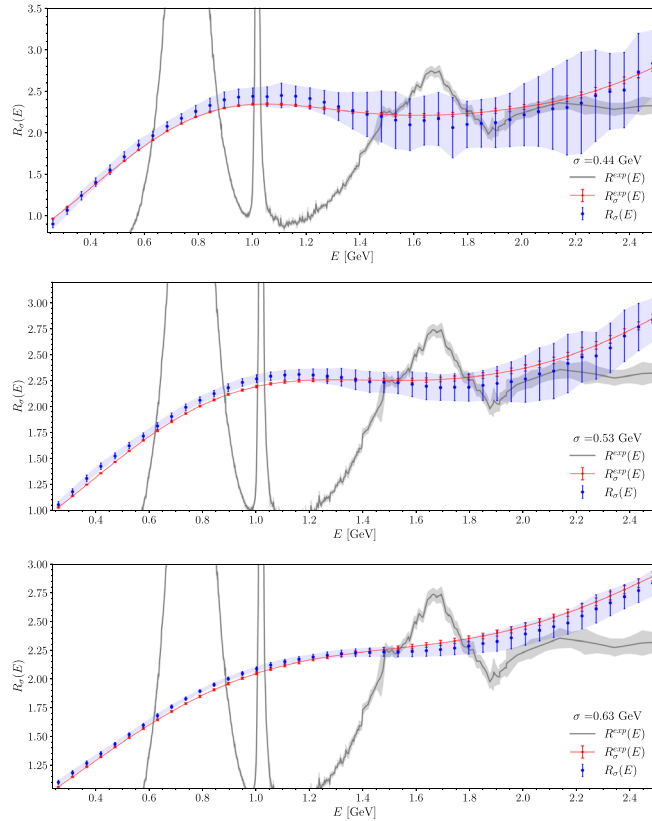


FIG. 3. Comparison of  $R_\sigma(E)$  (blue points) and  $R_\sigma^{\text{exp}}(E)$  (red points) as functions of  $E$  for  $\sigma = 0.44$  GeV (first row),  $\sigma = 0.53$  GeV (second row), and  $\sigma = 0.63$  GeV (third row).

extraction of spectral densities from Euclidean correlators is a challenging numerical problem, we consider the overall agreement between the theoretical and experimental data quite remarkable.

Although our theoretical errors,  $\Delta_\sigma(E)$ , are still substantially larger than the experimental ones,  $\Delta_\sigma^{\text{exp}}(E)$ , there is a tension between  $R_\sigma(E)$  and  $R_\sigma^{\text{exp}}(E)$  when the smearing Gaussian is centered in the region around the  $\rho$  resonance. This can be better appreciated in Fig. 5 where, for  $E < 1.3$  GeV, the plots on the left show the relative difference  $R_\sigma(E)/R_\sigma^{\text{exp}}(E) - 1$  while those on the right show the “pull”

$$\Sigma_\sigma(E) = \frac{R_\sigma(E) - R_\sigma^{\text{exp}}(E)}{\sqrt{[\Delta_\sigma(E)]^2 + [\Delta_\sigma^{\text{exp}}(E)]^2}}. \quad (7)$$

Before ascribing this tension, of about 3 standard deviations, to new physics or to underestimated experimental uncertainties a very important remark is in order.

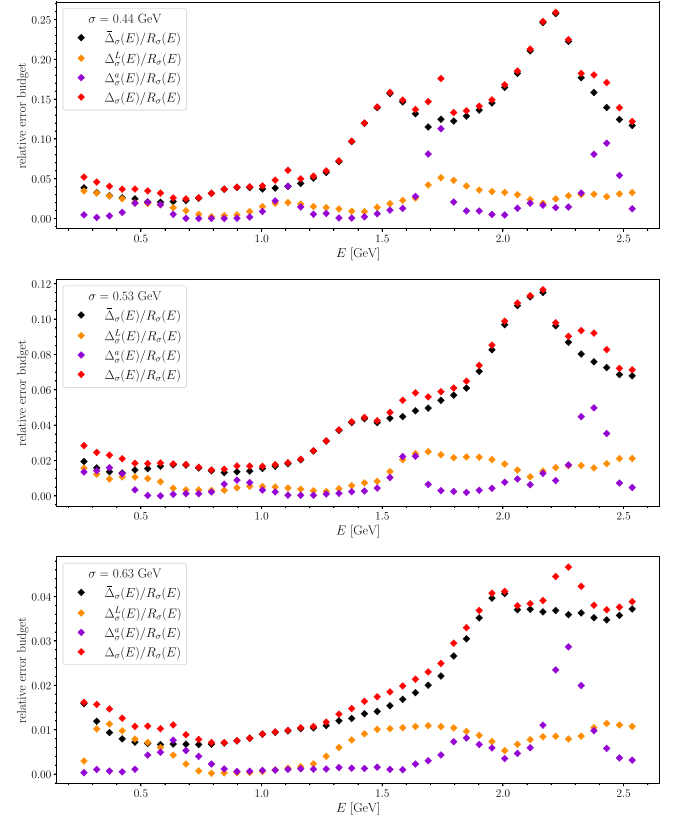


FIG. 4. Error budget for  $R_\sigma(E)$  at  $\sigma = 0.44$  GeV (first row),  $\sigma = 0.53$  GeV (second row), and  $\sigma = 0.63$  GeV (third row). The red points correspond to the total relative error,  $\Delta_\sigma(E)/R_\sigma(E)$ . The black points are the statistical errors combined in quadrature with the systematic errors coming from the spectral reconstruction algorithm,  $\bar{\Delta}_\sigma(E)/R_\sigma(E)$ . The violet and orange points are, respectively, our estimates of the relative systematic errors associated with the continuum extrapolations,  $\Delta_\sigma^d(E)/R_\sigma(E)$ , and finite volume effects,  $\Delta_\sigma^L(E)/R_\sigma(E)$ .

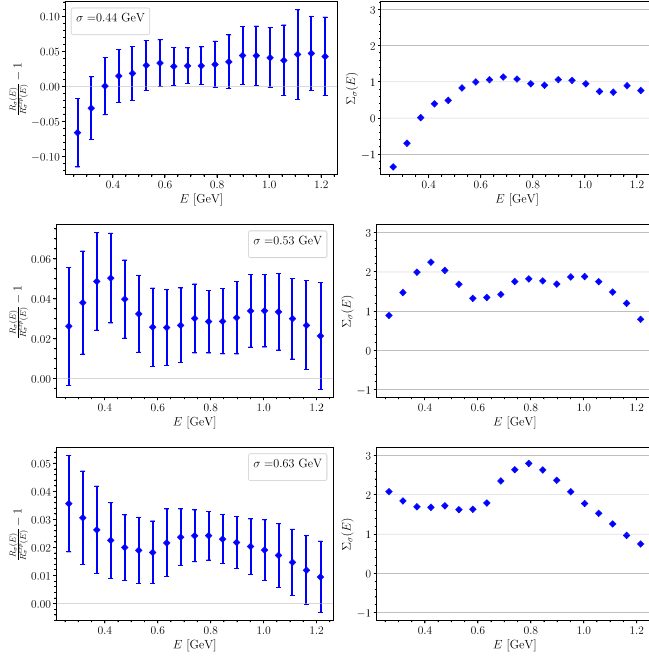


FIG. 5. Left plots: relative difference  $R_\sigma(E)/R_\sigma^{\text{exp}}(E) - 1$  as a function of the energy for  $\sigma = 0.44$  GeV (first row),  $\sigma = 0.53$  GeV (second row), and  $\sigma = 0.63$  GeV (third row). Right plots: the pull quantity  $\Sigma_\sigma(E)$ ; see Eq. (7) as a function of the energy for the three values of  $\sigma$ .

The calculation of  $R_\sigma(E)$  that we have performed in this study is an isosymmetric  $n_f = 2 + 1 + 1$  lattice QCD calculation, and therefore, we have not calculated yet, from first principles, the contributions to  $R_\sigma(E)$  coming from  $b$  quarks and from the QED and strong isospin breaking corrections. Concerning the  $b$ -quark contribution, if sizeable, this would represent a positive correction to  $R_\sigma(E)$  and thus, given the fact that  $R_\sigma^{\text{exp}}(E)$  is below  $R_\sigma(E)$  in the region in which these are in tension, it can only lead to an enhancement of the observed discrepancy. On the other hand, in the Supplemental Material [22] we provide numerical evidence that even the charm contribution is negligible for  $E < 1.5$  GeV at the current level of the theoretical precision. This is evident at  $E = 0.79$  GeV and  $\sigma = 0.63$  GeV, where we observe the largest tension, from the comparison of the first and third panels in Fig. 2. We therefore exclude that the observed tension can be ascribed to the  $b$ -quark contribution.

Isospin breaking effects definitely have to be evaluated from first principles:—Indeed, for very small values of  $\sigma$  very large isospin breaking effects have to be expected at certain values of  $E$ , e.g., at very low energy where the channel  $\pi^0 + \gamma$  opens in QCD + QED and also close to other thresholds (see Refs. [30,31]). Nevertheless, we notice that in order to explain the observed tension at  $E \sim 0.8$  GeV and  $\sigma \sim 0.6$  GeV an isospin breaking effect larger than 2% would be needed, and this is hard to reconcile with the first-principle lattice calculation performed in Ref. [5]

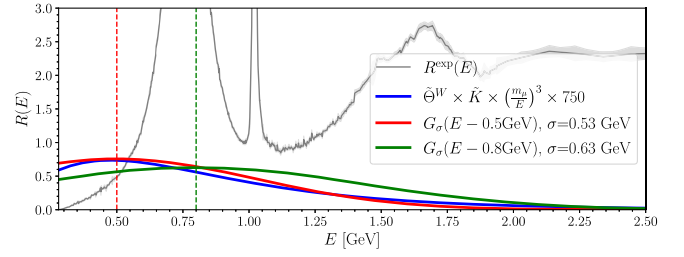


FIG. 6. The Gaussian kernels with central energy 0.5 GeV and width 0.53 GeV (red) and central energy 0.8 GeV and width 0.63 GeV (green) are compared with the intermediate window kernel  $\hat{\Theta}^W \times \hat{K} \times (E/m_\mu)^3$  (see, e.g., Ref. [7] for the explicit expression). The red Gaussian is centered at the peak of the intermediate window kernel (vertical red line) that is shown in blue and normalized such that the heights of the two peaks coincide. The green Gaussian is centered at the energy (vertical green line) where we observe the most significant tension (about 2.5% and 3 standard deviations) between  $R_\sigma(E)$  and  $R_\sigma^{\text{exp}}(E)$ . Using the red Gaussian we observe instead a 5% tension corresponding to 2.2 standard deviations; see Fig. 3.

of the isospin-breaking corrections on closely related quantities, in particular on  $a_\mu^{\text{HVP},W}$ . Indeed, the smearing kernel that in energy space defines  $a_\mu^{\text{HVP},W}$  is very similar in shape to the Gaussian kernel with central energy  $E = 0.5$  GeV and width  $\sigma = 0.53$  GeV (see Fig. 6), and the isospin-breaking effect on  $a_\mu^{\text{HVP},W}$  is found to be at the 2 permille level. We also note that, when  $R(E)$  is convoluted with the quite different (but always very much spread out in energy) kernels that define the long and short distance contributions to  $a_\mu^{\text{HVP}}$  (see Ref. [32]), the isospin-breaking corrections with respect to isosymmetric QCD remain very small, namely of about 1 permille [5] and 3 permille [33] respectively.

*Conclusions.*—We presented, for the first time, a non-perturbative theoretical study of the  $e^+e^-$  cross section into hadrons. We have calculated the  $R$  ratio convoluted with Gaussian smearing kernels of widths between 440 MeV and 630 MeV and center energies up to 2.5 GeV. We compared our first-principles theoretical results with the corresponding quantity obtained by using the KNT19 compilation [2] of  $R$ -ratio experimental data courteously provided by the authors.

For central energies of the smearing Gaussian in the region around the  $\rho$  resonance our results are sufficiently precise to let us observe a tension of about 3 standard deviations with experiments. Solid evidence of a significant discrepancy between theory and experiment already emerged also from the comparison of the lattice calculations [5,7,12,13] of the (window) contributions to  $a_\mu^{\text{HVP}}$  and the corresponding dispersive determinations [2]. Our results corroborate this evidence and, being totally unrelated to the muon  $g - 2$  experiment, highlight the fact that

the tension is between experimental measurements of the  $e^+e^-$  inclusive hadronic cross section and first-principles standard model theoretical calculations and are localized in a Gaussian energy bin of width  $\sigma \sim 600$  MeV and center energy  $E \sim 800$  MeV.

Although we argued that an isospin breaking corrections larger than 2% would be required to fully reconcile our lattice data with experiments, and that such a large correction is hardly conceivable in view of the few permille effects found in the related full and intermediate window contributions to  $a_\mu^{\text{HVP}}$  in Ref. [5], as a matter of fact, the phenomenological relevance of our theoretical results is partially reduced by the missing QED and strong isospin-breaking corrections.

At the same time, from the methodological perspective, the observed tension provides a solid numerical evidence of the fact that it is possible to study the  $R$  ratio in Gaussian energy bins on the lattice at the precision level required to perform precision tests of the standard model.

In future work on the subject we plan to substantially reduce the widths of the smearing Gaussians. Preliminary investigations make us confident on the possibility of studying  $R_\sigma(E)$  with  $\sigma \sim 200$  MeV by doubling the statistics on the isosymmetric QCD correlators already considered in this study. Moreover, we plan to compute from first principles the missing QED and strong isospin-breaking corrections to  $R_\sigma(E)$ .

We warmly thank A. Keshavarzi, D. Nomura, and T. Teubner, the authors of the KNT19 combination [2] of  $R$ -ratio experimental measurements, for kindly providing us their results. We thank all members of ETMC for the most enjoyable collaboration. N. T. warmly thanks L. Del Debbio, A. Lupo, and M. Panero for illuminating discussions on the Bayesian probabilistic interpretation of the method of Ref. [1]. We thank the developers of the QUDA [34–36] library for their continued support, without which the calculations for this project would not have been possible. S. B. and J. F. are supported by the H2020 project PRACE 6-IP (Grant Agreement No. 82376) and the EuroCC project (Grant Agreement No. 951740). We acknowledge support by the European Joint Doctorate program STIMULATE Grant Agreement No. 765048. P. D. acknowledges support from the European Unions Horizon 2020 research and innovation program under the Marie Skłodowska-Curie Grant Agreement No. 813942 (EuroPLEX) and also support from INFN under the research project INFN-QCDLAT. K. H. is supported by the Cyprus Research and Innovation Foundation under Contract No. POST-DOC/0718/0100, under Contract No. CULTURE-AWARD-YR/0220/0012, and by the EuroCC project (Grant Agreement No. 951740). R. F. and N. T. acknowledge partial support from the University of Tor Vergata program “Beyond Borders/Strong Interactions: from Lattice QCD to Strings, Branes and Holography.” F. S., G. G., and S. S. are supported by the

Italian Ministry of University and Research (MIUR) under Grant No. PRIN20172LNEEZ. F. S. and G. G. are supported by INFN under GRANT73/CALAT. This work is supported by the Deutsche Forschungsgemeinschaft (DFG, German Research Foundation) and the NSFC through the funds provided to the Sino-German Collaborative Research Center CRC 110 “Symmetries and the Emergence of Structure in QCD” (DFG Project-ID No. 196253076—TRR 110, NSFC Grant No. 12070131001). The authors gratefully acknowledge the Gauss Centre for Supercomputing e.V. for funding the project pr74yo by providing computing time on the GCS Supercomputer SuperMUC at Leibniz Supercomputing Centre, as well as computing time projects on the GCS supercomputers JUWELS Cluster and JUWELS Booster [37] at the Jülich Supercomputing Centre (JSC) and time granted by the John von Neumann Institute for Computing (NIC) on the supercomputers JURECA and JURECA Booster [38], also at JSC. Part of the results were created within the EA program of JUWELS Booster also with the help of the JUWELS Booster Project Team (JSC, Atos, ParTec, NVIDIA). We further acknowledge computing time granted on Piz Daint at Centro Svizzero di Calcolo Scientifico (CSCS) via the project with ID No. s702. The authors acknowledge the Texas Advanced Computing Center (TACC) at The University of Texas at Austin for providing HPC resources that have contributed to the research results. The authors gratefully acknowledge PRACE for awarding access to HAWK at HLRS within the project with ID No. Acid 4886.

---

\*Corresponding author.

nazario.tantalo@roma2.infn.it

- [1] M. Hansen, A. Lupo, and N. Tantalo, Extraction of spectral densities from lattice correlators, *Phys. Rev. D* **99**, 094508 (2019).
- [2] A. Keshavarzi, D. Nomura, and T. Teubner,  $g - 2$  of charged leptons,  $\alpha(m_z^2)$ , and the hyperfine splitting of muonium, *Phys. Rev. D* **101**, 014029 (2020).
- [3] N. Cabibbo, G. Parisi, and M. Testa, Hadron production in  $e^+e^-$  collisions, *Lett. Nuovo Cimento* **4S1**, 35 (1970).
- [4] T. Aoyama *et al.*, The anomalous magnetic moment of the muon in the standard model, *Phys. Rep.* **887**, 1 (2020).
- [5] S. Borsanyi *et al.*, Leading hadronic contribution to the muon magnetic moment from lattice QCD, *Nature (London)* **593**, 51 (2021).
- [6] R. Frezzotti, P. A. Grassi, S. Sint, and P. Weisz (Alpha Collaboration), Lattice QCD with a chirally twisted mass term, *J. High Energy Phys.* **08** (2001) 058.
- [7] C. Alexandrou *et al.*, Lattice calculation of the short and intermediate time-distance hadronic vacuum polarization contributions to the muon magnetic moment using twisted-mass fermions, *Phys. Rev. D* **107**, 074506 (2023).
- [8] J. Bulava, M. T. Hansen, M. W. Hansen, A. Patella, and N. Tantalo, Inclusive rates from smeared spectral densities in the two-dimensional O(3) non-linear  $\sigma$ -model, *J. High Energy Phys.* **07** (2022) 034.

- [9] J. Bulava, The spectral reconstruction of inclusive rates, *Proc. Sci. LATTICE2022* (**2023**) 231 [arXiv:2301.04072].
- [10] R. A. Bertlmann, G. Launer, and E. de Rafael, Gaussian sum rules in quantum chromodynamics and local duality, *Nucl. Phys.* **B250**, 61 (1985).
- [11] F. V. Ignatov *et al.* (CMD-3 Collaboration), Measurement of the  $e^+e^- \rightarrow \pi^+\pi^-$  cross section from threshold to 1.2 GeV with the CMD-3 detector, arXiv:2302.08834.
- [12] C. T. H. Davies *et al.* (Fermilab Lattice, HPQCD, and MILC Collaborations), Windows on the hadronic vacuum polarisation contribution to the muon anomalous magnetic moment, *Phys. Rev. D* **106**, 074509 (2022).
- [13] M. Cè *et al.*, Window observable for the hadronic vacuum polarization contribution to the muon  $g-2$  from lattice QCD, *Phys. Rev. D* **106**, 114502 (2022).
- [14] T. Blum, P. A. Boyle, V. Gülpers, T. Izubuchi, L. Jin, C. Jung, A. Jüttner, C. Lehner, A. Portelli, and J. T. Tsang (RBC and UKQCD Collaborations), Calculation of the Hadronic Vacuum Polarization Contribution to the Muon Anomalous Magnetic Moment, *Phys. Rev. Lett.* **121**, 022003 (2018).
- [15] G. Colangelo, A. X. El-Khadra, M. Hoferichter, A. Keshavarzi, C. Lehner, P. Stoffer, and T. Teubner, Data-driven evaluations of Euclidean windows to scrutinize hadronic vacuum polarization, *Phys. Lett. B* **833**, 137313 (2022).
- [16] An alternative, but closely related strategy, has recently been proposed in Ref. [17]. We also point out to the readers familiar with the Bayesian literature on the subject that, by using the results of Ref. [18], the method of Ref. [1] can be understood within the language of Gaussian processes; see, e.g., Refs. [19–21] and the explanation provided in the Supplemental Material [22], which also includes Refs. [23–25]. See also the recent review [26] for a critical discussion of the different methods, with an emphasis on those based on Bayesian inference.
- [17] D. Boito, M. Golterman, K. Maltman, and S. Peris, Spectral-weight sum rules for the hadronic vacuum polarization, *Phys. Rev. D* **107**, 034512 (2023).
- [18] A. Valentine and M. Sambridge, Gaussian process models-I. A framework for probabilistic continuous inverse theory, *Geophys. J. Int.* **220**, 1632 (2020).
- [19] J. Horak, J. M. Pawłowski, J. Rodríguez-Quintero, J. Turnwald, J. M. Urban, N. Wink, and S. Zafeiropoulos, Reconstructing QCD spectral functions with Gaussian processes, *Phys. Rev. D* **105**, 036014 (2022).
- [20] L. Del Debbio, T. Giani, and M. Wilson, Bayesian approach to inverse problems: An application to NNPDF closure testing, *Eur. Phys. J. C* **82**, 330 (2022).
- [21] A. Candido, L. Del Debbio, T. Giani, and G. Petrillo, Inverse problems in PDF determinations, *Proc. Sci. LATTICE2022* (**2023**) 098 [arXiv:2302.14731].
- [22] See Supplemental Material at <http://link.aps.org/supplemental/10.1103/PhysRevLett.130.241901> for details.
- [23] J. C. A. Barata and K. Fredenhagen, Particle scattering in Euclidean lattice field theories, *Commun. Math. Phys.* **138**, 507 (1991).
- [24] G. Bailas, S. Hashimoto, and T. Ishikawa, Reconstruction of smeared spectral function from Euclidean correlation functions, *Prog. Theor. Exp. Phys.* **2020**, 043B07 (2020).
- [25] G. Backus and F. Gilbert, The resolving power of gross earth data, *Geophys. J. Int.* **16**, 169 (1968).
- [26] A. Rothkopf, Inverse problems, real-time dynamics and lattice simulations, *EPJ Web Conf.* **274**, 01004 (2022).
- [27] R. Frezzotti and G. C. Rossi, Chirally improving Wilson fermions. II. Four-quark operators, *J. High Energy Phys.* **10** (2004) 070.
- [28] R. Frezzotti and G. C. Rossi, Chirally improving Wilson fermions. 1. O(a) improvement, *J. High Energy Phys.* **08** (2004) 007.
- [29] R. Frezzotti, G. Martinelli, M. Papinutto, and G. C. Rossi, Reducing cutoff effects in maximally twisted lattice QCD close to the chiral limit, *J. High Energy Phys.* **04** (2006) 038.
- [30] G. Colangelo, M. Hoferichter, B. Kubis, and P. Stoffer, Isospin-breaking effects in the two-pion contribution to hadronic vacuum polarization, *J. High Energy Phys.* **10** (2022) 032.
- [31] M. Hoferichter, G. Colangelo, B.-L. Hoid, B. Kubis, J. R. de Elvira, D. Stamen, and P. Stoffer, Chiral extrapolation of hadronic vacuum polarization and isospin-breaking corrections, *Proc. Sci. LATTICE2022* (**2022**) 316 [arXiv:2210.11904].
- [32] C. Alexandrou *et al.*, Short & intermediate distance HVP contributions to muon  $g-2$ : SM (lattice) prediction versus  $e^+e^-$  annihilation data, arXiv:2212.10490.
- [33] R. V. Harlander and M. Steinhauser, rhad: A program for the evaluation of the hadronic  $r$ -ratio in the perturbative regime of QCD, *Comput. Phys. Commun.* **153**, 244 (2003).
- [34] M. A. Clark, R. Babich, K. Barros, R. C. Brower, and C. Rebbi, Solving lattice QCD systems of equations using mixed precision solvers on GPUs, *Comput. Phys. Commun.* **181**, 1517 (2010).
- [35] R. Babich, G. Shi, M. Clark, R. Brower, B. Joó, and S. Gottlieb, Scaling lattice QCD beyond 100 GPUs, in *SC'11: Proceedings of 2011 International Conference for High Performance Computing, Networking, Storage and Analysis* (IEEE, New York, 2011), pp. 1–11.
- [36] M. A. Clark, B. Joó, A. Strelchenko, M. Cheng, A. Gambhir, and R. C. Brower, Accelerating lattice QCD multigrid on GPUs using fine-grained parallelization, in *SC'16: Proceedings of the International Conference for High Performance Computing, Networking, Storage and Analysis* (IEEE, New York, 2016), pp. 795–806.
- [37] D. Krause, JUWELS: Modular Tier-0/1 supercomputer at the Jülich supercomputing centre, *J. Large-Scale Res. Facil.* **5**, A135 (2019).
- [38] D. Krause and P. Thörnig, JURECA: Modular supercomputer at the Jülich supercomputing centre, *J. Large-Scale Res. Facil.* **4**, A132 (2018).